STRUCTURAL BEHAVIOR OF THE SOUTH ROAD CURVED GIRDER BRIDGE

Robert F. Victor, Bureau of Highways, Connecticut Department of Transportation

Presented are the major results of a field study that included the field testing of a horizontally curved, steel-girder bridge of welded I-girder and concrete slab construction and the subsequent analyses made to determine the analytical stresses and deformations that would match those produced by the construction and test vehicle static loadings. Analyses were made with the approximate and curved grid methods with variations in the stiffness parameters of moments of inertia and torsional constants. A comparison with slab-load experimental data revealed that the dead-load flexural stresses and vertical deflections could be predicted by both methods. Dead-load response was found to be relatively independent both of the torisonal constants of the girder members and of the transverse stiffness of the structure (moments of inertia of diaphragms and slab). The live-load tests were conducted with an FHWA test vehicle that was driven along 5 different lanes. The approximate method could not predict flexural stresses or vertical deflections, nor could either method be made to give lateral bending stresses. Rotations could not be predicted by the grid method. Other effects investigated were nonlinear stresses due to wheel contact and web slenderness.

•WITH EMPHASIS in recent years on structures of clean, aesthetically pleasing lines and surfaces, horizontally curved girders have increasingly been used for structures on difficult curved alignment. Two factors tending to increase their use have been the subjugation of bridge alignment considerations to roadway alignment considerations and the increased span lengths of overpass structures over divided highways, resulting from the elimination of side piers for traffic safety. When the overpassing roadways have moderate to sharp curvature, continuous spans for the bridge structures would be ruled out and simple spans with their greater girder depths and large slab overhangs would be required unless continuous curved girders were utilized.

In spite of the increased number of curved bridges built in the past few years and the various analytical methods advanced to explain their behavior (1, 2, 3, 4, 5), the stress distribution in a structure with horizontally curved, welded I-girders remains the subject of conjecture; and thus improvements to these methods await the investigation of the structural behavior of various curved girder bridges.

In the design of any bridge, it is desirable to know the stresses and deflections that occur in any part of the structure so that plate dimensions of girders can be held to a minimum consistent with permissible stresses and deflections. Realistically, any analytical method used in practice must employ simplifications and approximations so that design times can be shortened. Any improvements in the analytical methods must satisfy the criteria of significant improvement in economy or improvements in structural performance or both.

It is to this last statement that this paper is addressed. Would the knowledge of the structural response of a full-scale curved girder bridge to dead and live loads be of use in establishing criteria to improve analytical methods used in curved-girder design? This paper is concerned with the interpretation of data from a program of dead- and live-load testing and a comparison of these data with two analytical methods, the "approximate method" (3, 6) and a curved grid program (2) currently used by the Bridge Design Section of the Connecticut Department of Transportation. It is hoped that the information presented here will contribute to a better understanding of the structural behavior and help to determine criteria for the design of curved-girder bridges.

EXPERIMENTAL BRIDGE

Designed by Edward F. Hubert of the Connecticut Department of Transportation, the South Road grade separation is the first curved-girder bridge in Connecticut. Carrying a 2-lane local road over Interstate 84 in Farmington (Fig. 1), the structure has a 40-ft roadway with a certerline radius of 1,043 ft and is 2-span continuous (175 ft each on centerline South Road).

In cross section (Fig. 2), the bridge has 3 steel girders 19.25 ft on centers. The girders vary in depth from 7 ft at midspan to 12 ft at the pier. Cross frames are 17.5 ft on centers, at the tenth-points of the span, and are in the form of K-bracing with a separate top chord member (Fig. 2). Lateral bracing frames in at every other cross-frame connection (Fig. 3). The detailed girder data are shown in Figure 4. The reinforced concrete deck is haunched over the girders with a $9\frac{1}{2}$-in. minimum thickness between girders. Details of sidewalk, parapet, wearing surface, and protective fencing are shown in Figure 2.

The structure was designed as noncomposite by using the approximate method of analysis (3, 6) to determine the stresses in the girders and to proportion plate sizes accordingly. A 3-girder system was selected principally for fabrication economy; substructure units were set radially. Girder depths were set somewhat deeper than the minimum permitted of L/25 (7) to offset the expected increased deflection of the outside girder and to provide a greater overall rigidity.

SCOPE

The girders were instrumented at 3 sections along the bridge for both the dead- and live-load testing. Four cross frames had strain gauges for the dead-load testing; for the live-load testing, only 2 cross frames had gauges (Fig. 5).

Deflections were observed in the dead-load testing (Fig. 6) at 3 points on each girder in each span. Points in one span are symmetrical to those in the other. Deflections and bottom-flange rotations for the live-load testing were obtained at locations shown in Figure 5. The location of the pair of deflection gauges at section 7, girder 1, is symmetrical to that of section 9, girder 1. Girder 1 had more deflection gauges so that a determination could be made of its deflected shape under load.

The loads for the dead-load testing consisted of formwork, slab, wearing surface, sidewalk, and parapets. Because of the many problems encountered and the inconsistencies in the results of this testing, all but a small portion of the slab-load results were disregarded (8). The latter experimental stresses are compared to those produced by the approximate method (3) and a curved grid analysis (2).

The live load was an FHWA test vehicle that closely simulated an HS20 truck. Both static-position and crawl-run data were obtained by oscillograph recordings. However, because the static-position test results are somewhat unreliable because of drift, the crawl-run test data were developed more fully and were used almost exclusively for comparison with analytical values. Live-load responses investigated are as follows:

1. The variation of flexural and lateral bending stresses with location of the FHWA test vehicle,
2. The vertical deflections and torsional rotations of the bottom flanges with the passage of the test vehicle,
3. The stresses in the bottom angles of a pair of cross frames,
4. The variation of the distribution of moment among the 3 girders at a midspan cross section for the different lateral positions of the test vehicle,
5. The effect of stiffnesses of the various structural components (slab, cross frames, and girders) on the stress distribution in the structure, and
6. Localized secondary stress effects adjacent to the wheels of the test vehicle.

Figure 1. General bridge views.

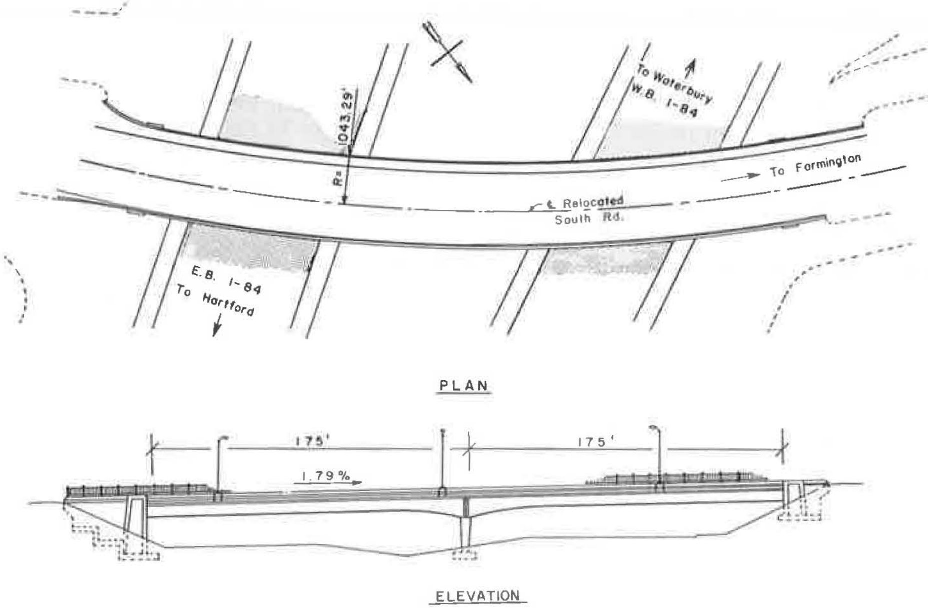

Figure 2. Typical bridge cross section.

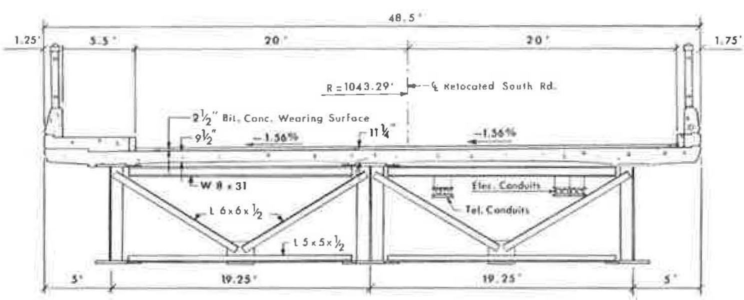

Figure 3. Half-framing plan (north span shown).

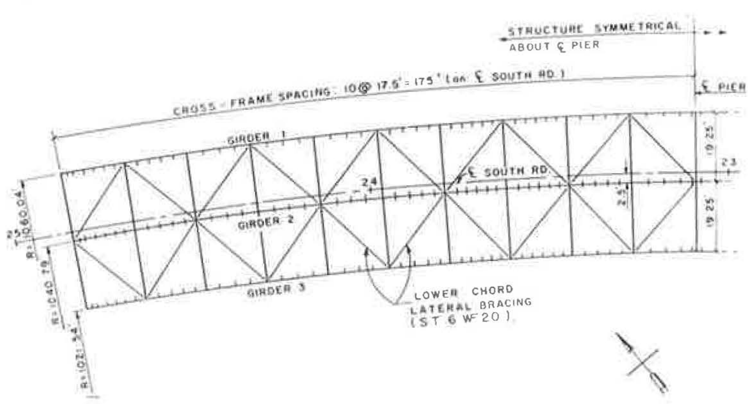

Figure 4. Girder data.

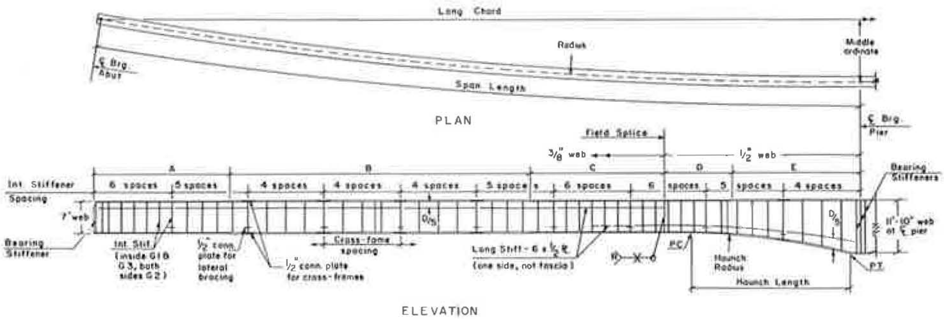

Girder	Span Length	Radius	Middle Ord.	Haunch Length	Haunch Radius	ASTM Des.	A Flange	A Length	B Flange	B Length	C Flange	C Length	ASTM Des.	D Flange	D Length	E Flange	E Length	C-Frame Spacing	Stiffeners Int.	Stiffeners Bearing
1	177.81	1060.04	14.88	40.00	167.93	A441M	30 x 1 5/8	31.00	30 x 2 5/16	70.00	30 x 1 5/8	31.00	A441M	30 x 1 5/8	16.00	30 x 2 1/2	29.81	17.78	10 x 5/8	14 x 1 1/4
2	174.58	1040.79	14.61	39.00	159.76	A441M	28 x 1 1/2	30.75	28 x 2	68.50	28 x 1 1/2	30.75	A441M	28 x 1 1/2	15.50	28 x 2 7/8	29.08	17.46	8 x 1/2	13 x 1 1/4
3	171.35	1021.54	14.34	38.00	151.80	A36	26 x 1 3/8	25.50	26 x 2 3/16	76.50	26 x 1 3/8	25.50	A441M	26 x 1 3/8	17.00	26 x 2 1/2	26.85	17.14	10 x 5/8	12 x 1 1/4

Note: Since design is non-composite, top and bottom flanges are the same.

Haunch Radius is to bottom of web.

Plate dimensions are in inches. Other dimensions are in feet.

Figure 5. Plan of grid model with gauge locations.

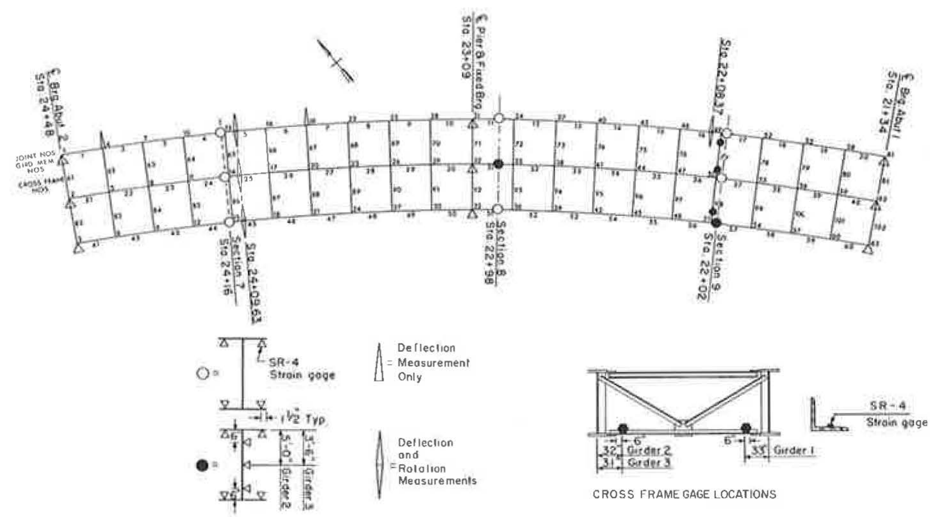

Figure 6. Slab pour sequence.

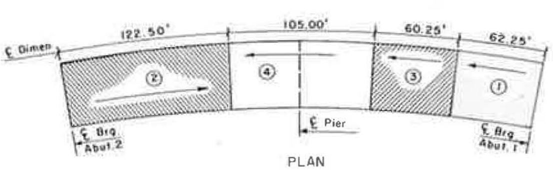

GIRDER	1	2	3
w (klf)	1.934	2.465	2.132

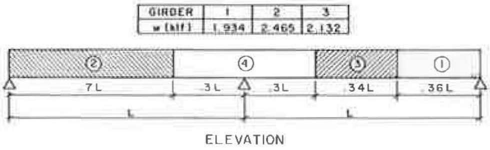

ANALYTICAL COMPARISON AND DISCUSSION OF DEAD LOAD

The purpose of the dead-load testing was to experimentally determine the stresses and deflections due to each increment of loading and to determine whether the analytical methods used in design would predict these stresses and deflections. If these stresses and deflections could not be determined with the parameters used in design, then what adjustments would be required to match the analytical values to the experimental?

Because of the experimental procedures followed, however, the dead-load data obtained are marginal (8). Although the experimental total stress is not known, the incremental loading stresses of slab pours 2, 3, and 4 were considered sufficiently accurate for comparison with analytical values.

Analytical Methods

The approximate method of analysis was originally proposed in a U. S. Steel Corporation report (3), and its use, with modifications, is illustrated in a U. S. Steel handbook (6). The following procedure was used in the analysis for each slab pour:

Each girder was analyzed (by using a plane frame computer program) as a straight 2-span continuous girder using the developed member lengths. Primary moments (6) were obtained by using the loads shown in Figure 6 for the load lengths indicated. Joints in the girder were located at cross-frame intersections so that moments could be compiled directly from output in order to facilitate computing V-loads, the shear loads induced on the inner and outer girders by torsion (6). In general, V-loads act downward in positive moment areas and upward in negative moment areas on girders outside the centerline of the girder system. For girders inside the centerline, the opposite is true.

For a 3-girder system, the V-loads are both equal and opposite for inner and outer girder. These loads are then input along with the slab loads to obtain the final shears, moments, and deflections of girders 1 and 3.

At this point, a lateral bending analysis is made of the flanges using the lateral-force magnitudes, M/R, at the cross-frame locations. The lateral force used in the analysis has an assumed straight-line variation from one cross frame to the next, and the computer program uses a reduced stiffness matrix (just the slope-deflection coefficients for rotations) to determine the lateral-bending moments.

The grid method was derived from and uses (with modifications) the stiffness equations for curved beams reported by Lavelle and Boick (2). For analysis, the structure is reduced to a gridwork of one-dimensional prismatic members consisting of curved grid members and diaphragm members that may be idealized as beams or trusses (5). The grid is analyzed by a standard analysis procedure termed the stiffness or equilibrium method. The method uses the slope-deflection coefficients for bending stiffnesses of a member and a torsional stiffness coefficient for twisting of a member. The member stiffness matrices thus formed are then transformed from the member-oriented axes to the structure-oriented axes by rotation matrices. The upper-band portion of the structure stiffness matrix is then generated preparatory to solution by Cholesky's square root method.

The computer program used for analysis generates structure geometry from input of the parameters of girder radii, span lengths, and diaphragm spacing. Members are then assigned properties of moments of inertia and torsional constants. Solution of equations (described earlier) is obtained by use of the Cholesky square root method that gives the structure displacements due to an applied loading. The displacements are then used to obtain the member end actions (shear, torque, and moment) for each member.

The flexural stresses were then obtained by hand calculation. The moments, shears, and applied loading from a lateral bending analysis (using girder torques instead of M/R quantities) were used to obtain, also by hand calculation, the lateral bending stresses at the gauge locations.

Flexural Stresses

The dead-load stresses were compared for slab pours 2, 3, and 4 at various gauge locations. Agreement with computed stresses was in many cases poor when gauges had drifted appreciably between pours. For gauges that remained relatively stable, results were generally better. More intensively examined were girder 2 at section 8 and girder 3 at section 9. Those gauge locations had strain gauges on the web and could give a better idea of stress distribution. The results are shown in Figures 7 and 8. Figure 7 shows that approximate, grid, and experimental stresses agree fairly well. The top-flange stresses for pours 2 and 3 are out of line with the other two but in these cases the top flange was exposed to heating by sunlight. When the top flange was finally covered in pour 4, that effect did not exist. No stresses can be presented for the lower half of the girder at this location because those gauges were inoperative. In all cases noncomposite section properties were used because the analytical stresses and deflections would generally be less than the experimental if partial composite action from previous pours is taken into account.

Figure 8 shows that results are less certain because the gauge at the center of the web had drifted badly and was unreliable (along with the top-flange gauges). Stresses from pour 4 were too small to be measured. The stress distribution shown in Figure 8 is based on the assumption that the strain gauges involved did not drift appreciably from the previous pour. Where the concrete is over the gauge location, the top-flange stress drops to less than that of the top-web gauge. This effect could be caused by shear lag in the wide flanges (9, 10); however, more gauges on the top flange would be needed to verify this effect. Consistent departure from straight-line stress variation across narrow flanges has been observed in other bridges (11) without apparent explanation.

Vertical Deflections

Figure 9 shows girder deflections for the total of all pours; Figure 10 shows girder deflections for slab pour 2. Similar results were obtained for pours 1, 3, and 4 but pour 2 gives the largest deflections.

Comparing analytical with experimental deflections shows some unusual results. For the relatively "clean" (i.e., the least effects from partial composite action) structure of slab pour 2, the analytical values are consistent with those of the experimental. Figure 9 (the total slab load deflection) shows that the deflected shape of the structure is the sum of construction deflections rather than the total load applied to a weightless elastic structure. The greater total deflections in the north span would seem to be a result of partial composite action of slab pour 2 that prevented the equaling of deflections in both spans.

In attempting to reproduce the various experimental dead-load deflections with the grid program, we used various combinations of properties: noncomposite, noncomposite with transverse slab stiffness, and composite analyses. Inclusion of transverse slab stiffness is simply adding the section properties of the slab to those of the cross frames. The torsion constant for a composite section was computed as $\Sigma(\frac{1}{3}bt^3)/n$. Inclusion of transverse slab stiffness decreased the maximum deflection by 4 percent; inclusion of composite action reduced the noncomposite maximum deflection by 28 percent. However, the composite analysis produced deflections that were too small in comparison to those measured. Of interest also is the fact that in this structure the diaphragms are cross frames. If these cross frames are idealized as trusses instead of beams, the end actions should be different for a given set of unit deformations (member stiffnesses) (5), thus conceivably changing the structure response. However, this modification changed little. As found in live-load analysis, the structure response is highly insensitive to changes in transverse stiffness.

Also found is the fact that the response of this structure is very insensitive to the torsional constant. Torsional constants used ranged from approximately 200 in.^{4} ($\Sigma \frac{1}{3}bt^3$) to 90,000 in.^{4} for girder members. Negligible variation was noted in analytical response (8).

Lateral-Bending Stresses

Only some general observations can be made about lateral-bending stresses because experimental values were inconclusive. In all cases, experimental stresses were greater in magnitude than predicted. Interaction of formwork and top flanges is not

Figure 7. Dead-load stress distribution at section 8, girder 2.

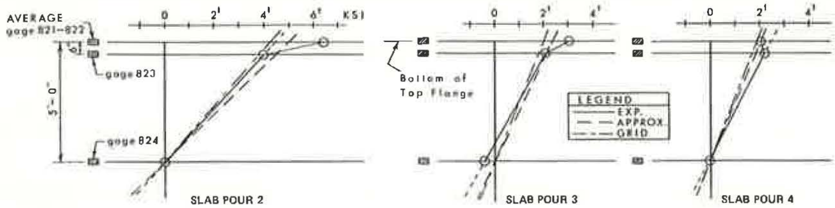

Figure 8. Dead-load stress distribution at section 9, girder 3.

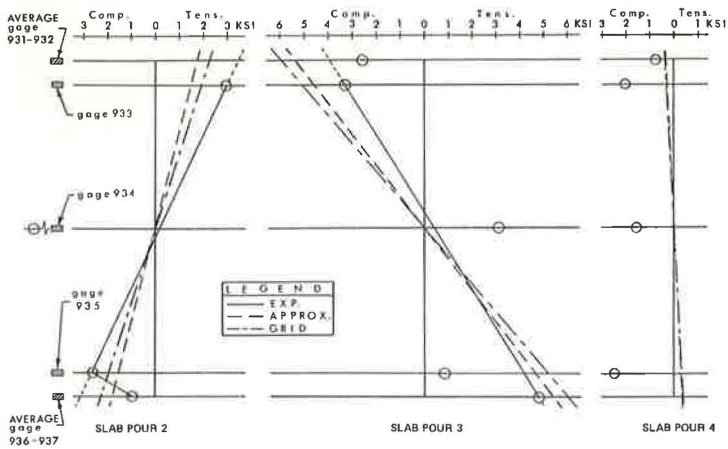

Figure 9. Total slab load deflection.

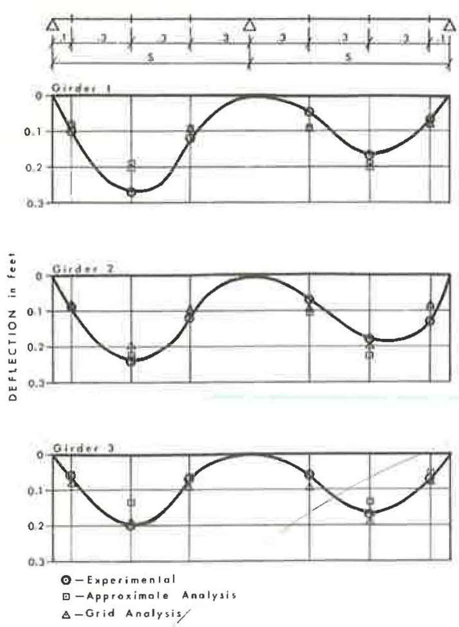

Figure 10. Pour 2 slab load deflection.

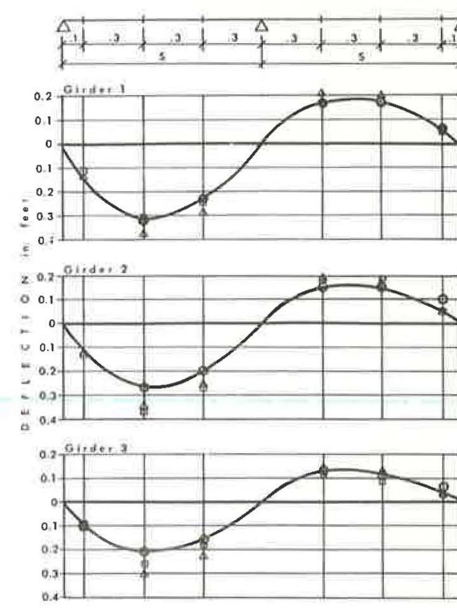

known but might have some effect because it laterally restrains the top flanges. With a series of slab pours, the top flange is unable to bend laterally under the hardened concrete slab; therefore, lateral-bending stresses under this slab should be zero for future loadings. Thus, these conditions of lateral restraint would seem to invalidate the lateral-bending analysis for reproducing experimental stresses.

ANALYTICAL COMPARISON AND DISCUSSION OF LIVE LOAD

Analytical Methods

The approximate method used for live-load analysis is nearly identical to that used for the dead-load analysis. Because the grid method was used as the main tool of analysis, the approximate method was confined to the noncomposite (the design basis) and the completely composite cases. No lateral-bending analysis was done in conjunction with this method. The method of applying the wheel loads of the test vehicle to the structure was the same for both the approximate and the grid methods. Wheel loads were distributed on a simple-span basis to adjacent joints (the intersections of girders and diaphragms).

The grid method is basically that described for dead-load analysis. Many different combinations of section properties were used in trying to reproduce experimental response. Composite sections used varied the parameters of modular ratio and slab widths. Torsional constants were computed as $\Sigma \frac{1}{3}bt^3$ until the entire width of slab with parapets was used. Torsional constants were then increased arbitrarily until experimental vertical deflections were matched. Transverse slab stiffness was tried both with and without the cross frames as diaphragm members.

The basic grid program was altered to increment the test vehicle along the structure in each of the lanes and to output the resulting stresses at the gauge locations (including lateral-bending stresses). Each position constitutes an alignment of front axle with diaphragm line. Diaphragm lines are numbered as their intersection with girder 1 (Fig. 5). Thus, for example, position 3-16 means lane 3, front axle at diaphragm members 66 and 87 (Fig. 5).

As data reduction proceeded, experimental results were compared to noncomposite grid analyses. From the resulting deflections and stresses, it was evident that more stiffness and strength would be needed to match the experimental results. Various composite sections were used: first, with AASHO criteria (7); second, with full slab width, modular ratio reduced to 5, parapets and sidewalk included in section properties of girders 1 and 3, and complete composite action included in the negative moment area; third, with torsional constant increased to 60,000 in.^{4} for each girder member; and, fourth, with preceding torsional constant changed to 90,000 in.^{4}.

Stress Distribution

The live-load stress distribution in the positive moment areas is basically linear with some small variation especially from web to flange (Fig. 11). In general, stress distribution across a moderately wide flange of a welded girder is nonlinear (9, 10, 11). Hence, for the flange gauge positions chosen, the measured stresses would not necessarily line up with those in the web.

In the negative moment area, the stress distribution in each girder is nonlinear because of the deep web (Fig. 12), the greater portion of which is in compression. This nonlinearity not only is caused by the truck itself but exists because the web is initially deformed from welding vertical stiffeners and has laterally deflected from the dead load. Only one longitudinal stiffener was used in this location. A more linear stress distribution would probably result from the use of multiple stiffeners.

Figure 12 shows, for truck position 3-37, that there is no readily discernible stress distribution. This stress pattern (or lack of it) is always true when the truck's wheels are nearby (see also the stress distribution shown in Fig. 13). The flexure formula, Mc/I, does not appear to govern under the influence of contact stresses imposed by the concentrated wheel loads (12). Indeed, the greatest top-flange stress occurred when the wheels passed by the gauge location. For all locations, these top-flange stresses

Figure 11. Live-load stress distribution at section 9, girder 3.

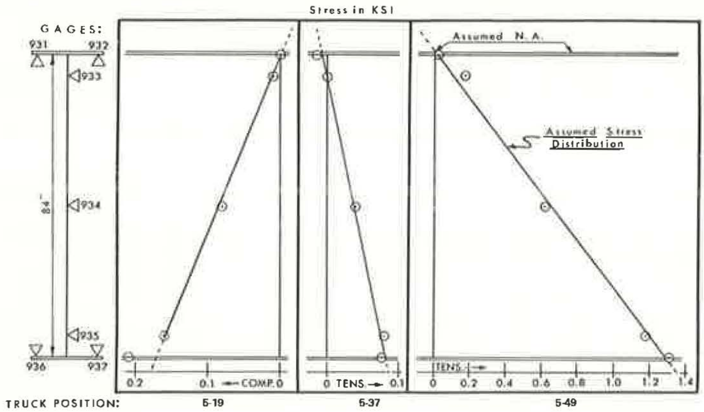

Figure 12. Live-load stress distribution at section 8, girder 2.

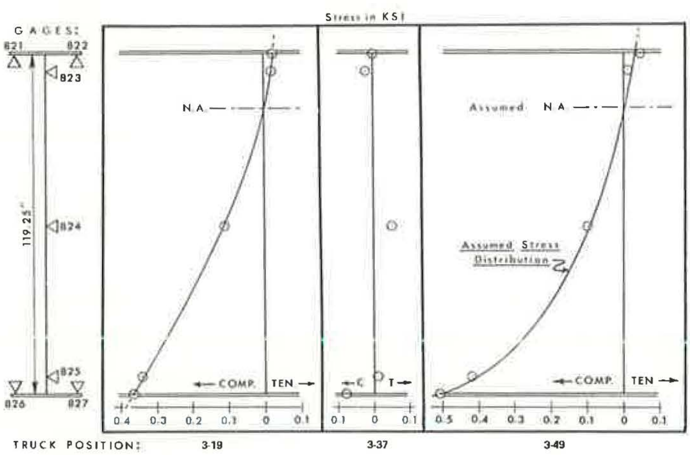

Figure 13. Typical stress behavior near wheels.

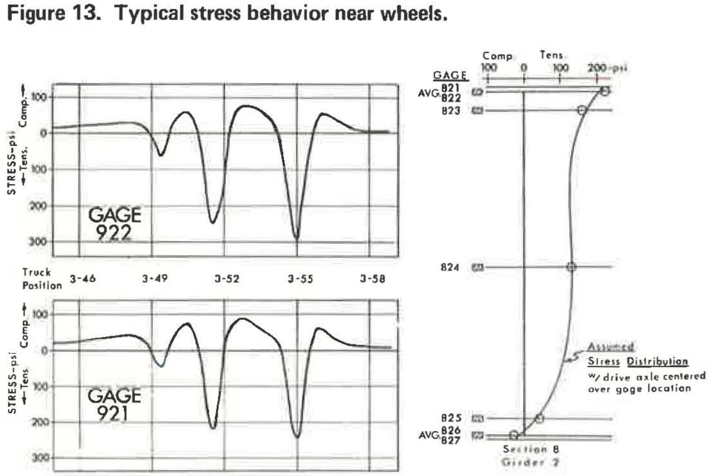

were always tensile. Figure 13 shows a typical top-flange gauge response. As the truck approaches the gauge location, there is a rise in the compressive stress; however, as the axle passes over the gauge location, there is a pronounced stress reversal. For truck position 3-55, a curved stress distribution is obtained with the neutral axis near the top of the slab for section 8, girder 2.

Neutral Axes and Modular Ratios

Apart from those truck locations where contact stresses dominated, neutral axes locations were generally at or near the top flange of the girder in all gauge locations. At section 9, girder 3, the neutral axis was finally assumed to be at the top of the top flange (because some small shifting of the neutral axis was noticed for various truck positions). For calculating a neutral axis location in the positive moment area, the following is needed: a modular ratio of 5; a slab width determined from the midpoints between the girders; for girder 1, inclusion of a portion of the parapet below the top of curb; and, for girder 3, inclusion of the sidewalk and the portion of parapet below the top of sidewalk. The top portion of the parapet was finally disregarded because it brought the neutral axes up too high. The parapets have vertical joints that are from 18 to 19 ft apart and are used to control shrinkage cracking. These vertical joints nullify the stiffening effect that the parapets otherwise might have.

A modular ratio of 5, used in the positive moment areas, is that which results from using the initial tangent modulus (based on the average 28-day cylinder strength of 5,200 psi). With the low stresses, rapid loading, and slab reinforcement, a modulus of elasticity of the slab or 5,800 ksi ($n = 5$) is certainly possible. In the negative moment area, the neutral axis at section 8, girder 2, was assumed to be about 19 in. below the bottom of the top flange (Fig. 12). If a modular ratio of 8 is assumed for the slab in tension, the computed neutral axis will be in the above location. Also if the reinforcing steel is considered separately from the concrete in computation for neutral axis location, a modular ratio of 9 is required for the concrete alone. With the low stresses encountered, we might logically expect to have the same modular ratio for both tension and compression because we are using the initial tangent modulus. However, the cracking of the concrete under shrinkage and permanent tensile stresses would account for this discontinuity in the slope of the stress-strain relation. With shrinkage cracking evident on the underside of the deck and under future repeated live-load action, the modular ratio in the tensile area should increase with time until perhaps the reinforcing steel acts alone. Composite action from the wearing surface was not considered.

Concrete Stresses

The concrete stresses from the three gauges were at all times very small. In comparing strains from the gauges on the bottom of the haunch with those on the adjacent top flange, we found that these strains were compatible. This compatibility would indicate complete, rather than partial, composite action.

Cross-Frame Stresses

The stresses produced by the readings from the cross-frame gauges show that these members are very active in the response of the structure. The maximum stresses produced were equal to those of the girder bottom-flange gauges (2 ksi maximum) and were found to be quite sensitive to the lateral position of the test vehicle.

If we consider the vertical deflections and rotations at section 7 to be representative of those at this particular cross frame, we find the bending stresses from analysis as a rigid frame to be very small under the maximum deformations. Thus, the stresses due to axial forces should predominate. With the gauges installed as shown in Figure 5, it is not possible to separate axial from bending stresses. Again when the measured vertical and rotational deformations from section 7 are used, it is apparent that the experimental stresses are consistent with the relative vertical deflections and especially the relative lateral deflections of the bottom flanges (the bottom flange rotations being used as a measure of lateral deflection) of the adjacent girders. The lateral deflections of the girders were not measured and could not be found from measured rotations.

Rotations

The rotations were measured on the bottom flange, which in general is not the average rotation of the girder. Because of the flexibility of the web, the bottom-flange rotations will be different from those of the slab. The bottom-flange rotations were found to be greater than the chord rotations of the slab (the relative girder deflections divided by the spacing) for girders 1 and 3 and less for girder 2. Generally, with the increasing torsional constants from the different grid analyses, the rotations decreased to the order of the experimental but in no way matched those values.

Vertical Deflections

With the increase in moments of inertia and torsional constants, the vertical deflections decreased noticeably for all girders, in proceeding from the noncomposite to completely composite analysis. With the increase in torsional constant to 90,000 $in.^4$ for each girder member, the deflections matched the experimental results from the gauges in the north span with the truck in that span (Figs. 14, 15, and 16). With the truck in the north span, the predicted vertical deflection for the deflectometer pair near section 9, girder 1, was consistently high (always an upward deflection). This predicted response was too high because a modular ratio of 5 was assumed in the negative moment area, but the neutral axis location at section 8, girder 2, shows that $n = 8$ with full slab width. Therefore, the area near the pier (negative moment area) is less stiff than assumed in analysis. If this reduced stiffness is used, all the predicted vertical deflections should match the experimental. Thus, the following parameters are needed for member properties in order to match analytical grid deflections to the measured values:

1. The full width of the slab;
2. An initial tangent modulus of elasticity for the modular ratio in the positive moment area (slab always in longitudinal compression);
3. A reduced modular ratio in the negative moment area (slab always in longitudinal tension) to account for transverse cracking;
4. A torsional constant of approximately 90,000 $in.^4$ for each girder member; and
5. Diaphragm stiffnesses with a moment of inertia of the slab equal to that calculated by $bh^3/12n$, taking the width of slab equal to the cross-frame spacing and the thickness equal to the minimum slab thickness and adding the moment of inertia of the cross frame computed as $\Sigma A\bar{y}^2$ of the top and bottom horizontal members (this approach works because the response of this structure is grossly insensitive to the variation in transverse stiffness).

Girder Stresses

The flange flexural stresses, measured as the average from the 2 flange gauges, were closely approximated by the grid method analysis, which matched the computed with the experimental deflections. Generally, for this particular analysis, computed stresses are higher than the experimental for bottom-flange stresses. If changes were made to the section properties as suggested for vertical deflections, these changes would be beneficial for comparing bottom-flange stresses because neutral axes would drop somewhat and lower the stresses. The changes in moments would be relatively small because moments are more insensitive to property changes than are the structure deflections and stresses.

Top-Flange Stresses

Flexural stresses were either zero or very small at sections 7 and 9 because the neutral axes are close to the top flanges at these sections. The lateral-bending stresses were always zero at all sections (any recorded difference was of the order of the

Figure 14. Girder behavior at section 7, lane 1.

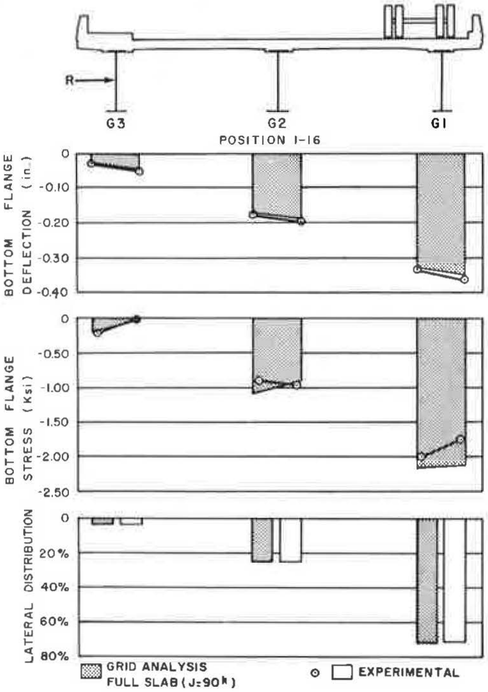

Figure 15. Girder behavior at section 7, lane 3.

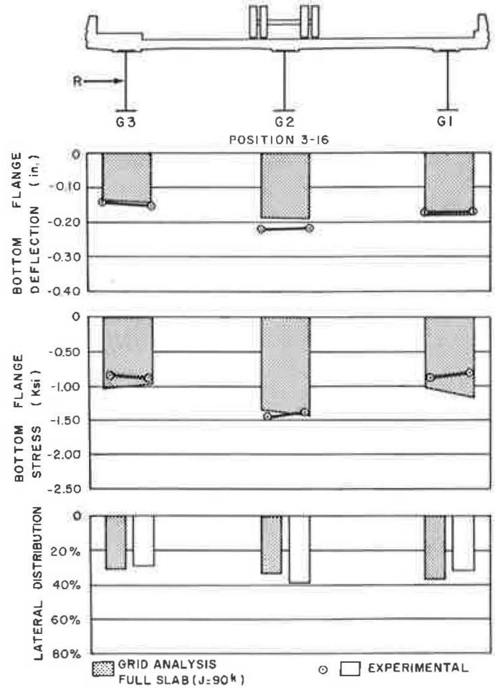

Figure 16. Girder behavior at section 7, lane 5.

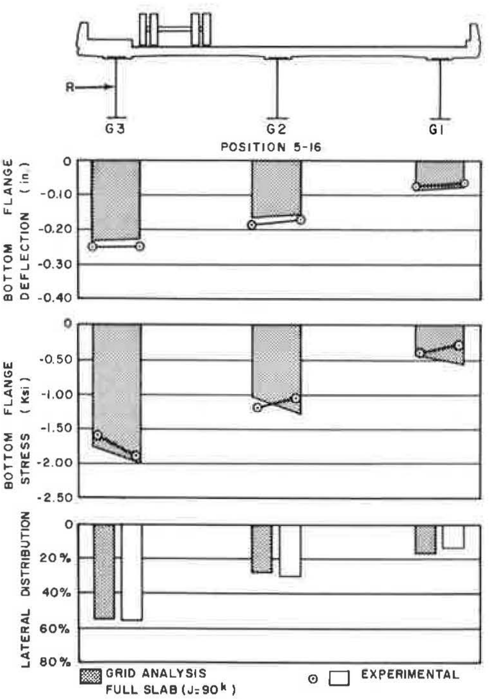

gauge accuracy) because the slab is infinitely stiff in its own plane (4). Most interesting is the variation in top-flange stresses when the wheels of the truck pass by the gauge location (Fig. 13). There is a complete live-load stress reversal at sections 7 and 9 and an increase in tensile stress at section 8. These stresses do not change the sign of the total stress in the top flanges (the dead-load stress is much larger) but, because of the compatibility of strain between the concrete and steel, the slab undergoes the stress reversal in the longitudinal direction. This reversal of stress with a moving truck would be very quick and more than likely contribute to the deterioration of the slab.

Bottom-Flange Stresses

The bottom-flange flexural stresses were consistently approached by the grid method as the stiffness parameters were increased to match the experimental vertical deflections with those of the grid analyses. The lateral-bending stresses were not approached by use of the girder torques in combination with the method in the U. S. Steel publications (3, 6). Other approaches for determining lateral-bending stresses seem too complex for design (13, 14), or the assumption of either total or zero torsional restraint at the ends of a member (15) is questionable. The most promising of the methods investigated for determining lateral bending stresses was that of Bouwkamp and Powell (11) in which the bottom flanges and web are represented as additional grid members. Thus, lateral-bending stresses can be computed from the member end moments on the bottom-flange members from this type of grid analysis.

Distribution Coefficients

Experimental distribution coefficients were determined by multiplying the average bottom-flange stress by the computed section modulus (which gives the experimental moment) and then by taking each moment as a percentage of the total moment at the test cross section. Results are shown for 3 lateral positions for the moments at section 7 in Figures 14, 15, and 16.

In obtaining the lateral distribution percentages, we found that the total moment at the cross section did not vary with the lateral position of the test vehicle. For each of the truck positions 1-16, 3-16, and 5-16 the total moment at section 7 was approximately 1,963 ft-kips. From the grid analysis, the total moment was 2,200 ft-kips. Use of section properties, which excluded the parapets, gave a total moment of 1,996 ft-kips.

Concluding Discussion

Throughout the live-load analysis, alterations were made to member properties in the grid method. This method was used as the main tool of analysis because it is a more sophisticated analytical tool than the approximate method. Although the approximate method with noncomposite section properties was used for design, it was found that it could not match the experimental live-load stresses and deflections. A distribution of the test vehicle's wheel loads to the joints (the intersections of girders and diaphragms) was done on a simple-span basis for all analyses. This initial distribution proved to be adequate for the grid method because this method is able to further distribute the applied loading. The total moment at the cross section is the same for both approximate and curved grid methods. Thus, the problem is one of lateral distribution of moment and deflection, and it would appear that an initial distribution of wheel loads, other than on a simple-span basis, is needed if the approximate method is to give valid flexural stresses and vertical deflections. With the grid method, the correct lateral distribution of moment and deflection was achieved by simply increasing the torsional constant.

The live-load vertical deflections and flexural stresses (and by implication, lateral distribution of moment) were matched to the experimental with the curved grid method. Torsional rotations were approached, but bottom-flange, lateral-bending stresses were not matched because these stresses are more closely related to the effects of nonuniform torsion. The approximate method, while giving the correct longitudinal distribution of moment, did not give a valid lateral distribution.

As a final analysis, the structure was assumed to be straight. It was found that the variation in response was at most 10 percent with most responses showing less variation. Thus, it may be said that the effect of curvature, for this structure, is to increase the stresses and deflections by not more than 10 percent.

REFERENCES

1. McManus, P. F., Nasir, G. A., and Culver, C. G. Horizontally Curved Girders—State of the Art. Proc. ASCE, Vol. 95, No. ST5, May 1969, p. 853.
2. Lavelle, F. H., and Boick, J. S. A Program to Analyze Curved Girder Bridges. Division of Engineering, Research, and Development, Univ. of Rhode Island, Kingston, Eng. Bull. 8, 1965.
3. Gordon Richardson and Associates. Analysis and Design of Horizontally Curved Steel Bridge Girders. U.S. Steel Corp., Struct. Rept., 1963.
4. Ketchek, K. Another Approach to Simplified Design of a Curved Steel Girder. AISC Eng. Jour., Vol. 6, No. 4, Oct. 1969.
5. Weissman, H. A. Straight-Element Grid Analysis of Horizontally Curved Beams. AISC Eng. Jour., Vol. 7, No. 2, April 1970.
6. Highway Structures Design Handbook. Vol. 1, Ch. 12, U.S. Steel Corp.
7. Standard Specifications for Highway Bridges. American Association of State Highway Officials, Washington, D.C., 1969.
8. Victor, R. F. Structural Behavior of the South Road Curved Girder Bridge. Bureau of Highways, Connecticut Department of Transportation, March 1971.
9. Beedle, L. S., et al. Structural Steel Design. Ronald Press Co., New York, 1964.
10. Bresler, B., and Lin, T. Y. Design of Steel Structures. John Wiley and Sons, New York, 1960.
11. Bouwkamp, J. G., and Powell, G. H. Structural Behavior of an Orthotropic Steel Deck Bridge. Department of Civil Eng., Univ. of California, Berkeley, Rept. SESM-67-27, 1967.
12. Seely, F. B., and Smith, J. O. Advanced Mechanics of Materials. John Wiley and Sons, New York, 1952.
13. Heins, C. P., Jr., and Seaburg, P. A. Torsion Analysis of Rolled Steel Sections. Bethlehem Steel Co., Steel Design File 13-A-1, 1964.
14. McManus, P. F., and Culver, C. G. Nonuniform Torsion of Composite Beams. Proc. ASCE, Vol. 95, No. ST6, June 1969, p. 1233.
15. Lyse, I., and Johnston, B. G. Structural Beams in Torsion. Trans., ASCE, Vol. 101, 1936, p. 857.